J Mater Sci (2006) 41:7741–7746
DOI 10.1007/s10853-006-0552-3

The role of partial grain boundary dislocations in grain boundary sliding and coupled grain boundary motion

Joshua Monk · Brian Hyde · Diana Farkas

Received: 31 March 2006 / Accepted: 8 June 2006 / Published online: 24 October 2006

Abstract We study the process of grain boundary sliding through the motion of grain boundary dislocations, utilizing molecular dynamics and embedded atom method (EAM) interatomic potentials. For a $\Sigma = 5$ [001]{310} symmetrical tilt boundary in bcc Fe, the sliding process was found to occur through the nucleation and glide of partial grain boundary dislocations, with a secondary grain boundary structure playing an important role in the sliding process. While the homogeneous nucleation of these grain boundary dislocations requires shear strain levels higher than 7%, preexisting grain boundary dislocations are shown to glide at applied shear levels of 1.5%. The glide of the dislocations results in coupled motion of the boundary in the directions parallel and perpendicular to itself. Finally, interstitial impurities and vacancies were introduced in the grain boundary to study the effects on the sliding resistance of the boundary. While vacancies and H interstitials act as preferred nucleation sites, C interstitials do not. Both hydrogen and C interstitials stop dislocation glide whereas vacancies do not. A detailed study of the dynamic properties of these dislocations is also presented.

Introduction

Grain boundaries play an important role in determining the mechanical properties of a polycrystalline material. In general, the mechanical properties of a grain boundary are highly dependent on their local atomic structure [1–4]. It has been shown that grain boundary sliding, the rigid translation of one grain over another one parallel to the GB interface, mediates plastic flow of polycrystalline materials, particularly at very small grain sizes [3, 5]. In particular, the motion of planar high-angle grain boundaries under the influence of a mechanical stress field can be attributed to the movement of the grain boundary dislocations which comprise the structure of the boundary [6–8]. The plastic deformation of grain boundaries is central to the understanding of a wide range of material behaviors, including super plasticity, and is critical in the mechanical behavior of nanostructured materials [1].

In analogy to the bulk deformation carried out microscopically by lattice dislocations, GB deformation occurs through the involvement of grain boundary dislocations. Given a boundary structure the Burgers vectors of the secondary GBDs, resulting from the dissociation of extrinsic GBDs, in general GBs can be predicted based on the DSC-lattice. An increasing CSL boundary index results in the decreasing magnitude of the corresponding DSC lattice basis vectors from which the Burgers vectors of the secondary grain boundary dislocations are determined [2]. Adding complexity to the process of grain boundary deformation, non-perfect grain boundary dislocations have been shown to appear in grain boundaries in a variety of materials [9, 10]. These defects have been termed ''disconnections'' in a more general sense. Interface motion can occur by the motion of disconnections.

The process of grain boundary sliding has been studied using a variety of simulation techniques. Computer simulations offer a unique tool for the study

J. Monk · B. Hyde · D. Farkas (✉)
Department of Materials Science and Engineering, Virginia Tech., 201 Holden, Blacksburg, VA 24061, USA
e-mail: diana@vt.edu

of the dynamic behavior of deformation processes such as grain boundary sliding by closely monitoring the evolution of the atomic structure [11–14].

Grain boundary sliding has been shown to occur along special and near special boundaries by the propagation of grain boundary dislocations [15]. Highly coincident boundaries contain intrinsic or primary dislocations that are an integral part of the boundary structure. Extrinsic or secondary grain boundary dislocations, which are created by reaction with lattice dislocations or other grain boundary sources, have been shown to significantly influence sliding resistance [8].

Sliding is often accompanied by migration of the boundary parallel to itself and has been shown to be associated with the movement of structural grain boundary dislocations [15]. This supports the idea that grain boundary sliding occurs due to the activation of definable grain boundary dislocations from within the boundary. In these models, the ratio of migration to sliding doesn't change depending on the source of the dislocations [14]. The grain boundary dislocations must have the same crystallographic parameters, and therefore be particular to certain grain boundary structures typically found in these special boundaries. The crystallography of the boundary fully determines the coupling constant between motion of the boundary parallel to itself and sliding.

The linkage between sliding and migration was studied by King and Smith [15]. Their theory invoked the motion of DSC dislocations and their associated steps in the boundary plane. Another important fact related to grain boundary configurations is that differing grain boundary structures may co-exist, separated by ''imperfect'' or non-DSC dislocations. The finding of such structural multiplicity was first made by Wang, Sutton and Vitek [16]. It is then possible to think that imperfect grain boundary dislocations may also play a role in grain boundary sliding.

Indeed, in recent work, we have studied the sliding of the $\Sigma = 5$ [001]{310}symmetrical tilt grain boundary in bcc iron due to shear deformation using embedded atom method (EAM) type atomic potentials [17]. In this boundary, sliding occurs by the nucleation and propagation of partial grain boundary dislocations. These are generated as pairs and are partial dislocations of the DSC lattice. The sliding process results in the migration of the boundary parallel to itself. The first pair of partial grain boundary dislocations emitted results in the creation of a region with a different grain boundary structure. We have shown that this structure corresponds to the second lowest energy structure for this boundary. The emission of the second pair of partial grain boundary dislocations restores the grain boundary structure to its lowest energy configuration.

These results show that low Σ grain boundaries slide by the nucleation and propagation of grain boundary dislocations. The mechanism results in coupled motion of the boundary parallel to itself as first suggested by Bishop et al [14]. The homogenous nucleation process requires a level of applied shear strain of 7–8%, which is higher than what is normally required for sliding, for example in nanocrystalline materials. In real materials these grain boundary dislocations may nucleate heterogeneously or may even be present as part of the equilibrium grain boundary structure, accommodating deviations from the exact CSL misorientation. Therefore in real materials the glide response of these dislocations may be more important than the nucleation process. The first objective of the present work is to study the glide process of these dislocations and the coupled resulting migration. Of particular interest are the levels of applied shear necessary to initiate glide of a preexisting dislocation.

Grain boundary segregation of impurities is known to have significant effects on grain boundary migration and sliding behavior. Segregation could thus change the structure of the grain boundary at the atomic level and play a role in the mechanisms of migration and sliding that operate in the boundary [18]. A similar role can be played by vacancies. In the present work, we performed a detailed investigation of the glide of these grain boundary dislocations and the effect of vacancies, H and C interstitial impurities on glide process [19].

Computational technique

The simulations are performed using computational cells that include a symmetrical tilt grain boundary characterized as $\Sigma = 5$, [001](310). The interatomic potentials used in this study are of the EAM type and are known to be adequate to describe the interaction of metals. For the case of bcc iron we have chosen the EAM potential by Simonelli et al. [20]. The potential predicts a cohesive energy of –4.28 eV/atom with a lattice constant of 0.2867 nm. This is an empirical potential and is used here as a model potential for a bcc metal.

For interactions involving carbon, we use the EAM potential developed by Ruda et al. [21]. The potential predicts correct trends for the dilute heat of solution and the effects of increasing carbon content on the equilibrium lattice parameter of the martensitic body centered tetragonal phase of Fe. For hydrogen interactions within the boundary we have selected a

similarly developed potential also developed by Ruda et al. [22]. These potentials are also empirical and are used here as model potentials for interstitial elements that segregate to the grain boundary.

A fixed region on both the top and bottom of the samples is utilized in order to apply shear deformation with all the interior atoms being free to move according to the potential. In the direction of the [001] tilt axis periodic boundary conditions were used with a periodicity of four times the lattice constant. This was done in order to avoid effects of the possible interaction of the impurities included in the boundary with their periodic images. In the other direction contained in the grain boundary plane we used free surface boundary conditions and a block size that contains 20 lattice periodicities. The reason we used a larger sample size in this direction is that this direction is the one in which grain boundary dislocations can glide. Therefore, the simulations block was the largest in this dimension in order to study the details of the dislocation glide process. We utilized standard molecular dynamics techniques and in order to isolate the structural effects from the thermal components of the glide behavior the temperature was kept at 1 K.

Results

The equilibrium structure of the boundary was studied and the minima of the grain boundary energy functional analyzed. The two lowest energy grain boundary structures obtained for this boundary are shown in Fig. 1. Dark and light atoms represent atoms that are on different levels above the plane of the figure. The two structures correspond to different translational states of the boundary [23]. After relaxation of the block using molecular statics the lowest energy for this grain boundary was found to be 1.109 J/m^2 (Fig. 1, left). Fig. 1 (right) shows an alternative grain boundary structure created by the removal of one plane of atoms located at the mirror plane and a rigid body displacement parallel to the boundary plane of 0.0241 nm. This structure is a local minimum of the potential energy for the bicrystal with a grain boundary energy of 1.322 J/m^2. This multiplicity of possible structures, and in particular the existence of a second lowest energy structure that is relatively close in energy to the global minimum, is important for the possibility of partial grain boundary dislocations. The structure in Fig. 1 (left) can be considered a grain boundary structure containing a translational fault. The energy of this translational fault is equal to the difference in the two grain boundary energies, in this case 211 mJ/m^2.

Nucleation of the dislocations

Figure 2 shows the process of nucleation of the grain boundary dislocation. The visualization in the figure at right is performed using forces on each atom to calculate the local shear stress corresponding to each atom in the boundary. It is seen that the equilibrium grain boundary structure contains some sites that are under tension for an applied shear strain of 7%. At this level of applied shear strain the stress is still uniformly distributed. However, at 7.5% applied shear strain a stress concentration develops at a particular site of the boundary and this site is where a pair of partial grain boundary dislocations nucleates. Note that as this pair nucleates there is a structural unit of the boundary characteristic of the higher grain boundary structure created between the two partials. As the partials move away from each other the region of grain boundary structure containing a translational fault increases. The driving force for these dislocations to move away from each other is the applied shear stress which will induce glide of the two partials in opposite directions.

The homogeneous nucleation of these dislocations requires a high shear stress, with the first stress concentration appearing at 7.5% shear strain in one of the structural units of the boundary. Further accumulation

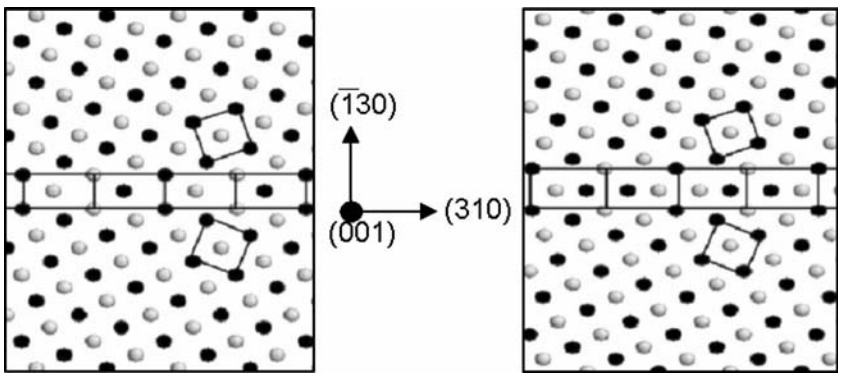

Fig. 1 The two lowest energy grain boundary structures. The structure on the left is the ground state and the one on the right is 211 mJ/m2 higher

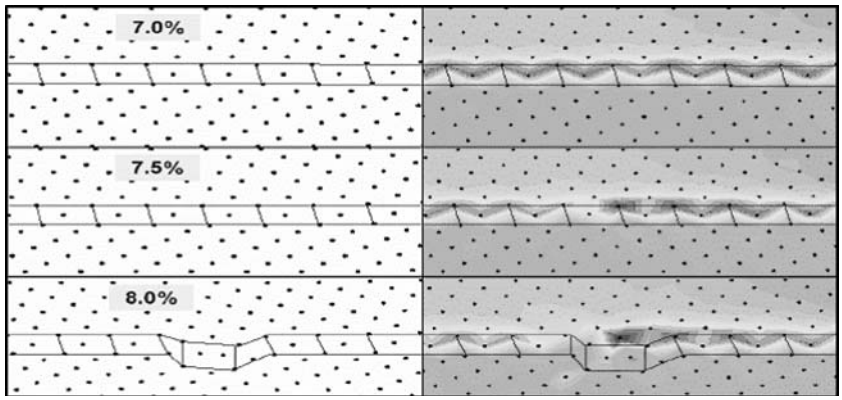

Fig. 2 The process of nucleation of a pair of partial grain boundary dislocations. The visualization on the right utilizes shading according to the local hydrostatic stress state for each atom. The darker shades correspond to regions under compression. As the pair moves away from each other a region of the higher grain boundary structure is created between them

of stress in the particular unit results in the nucleation of a pair of partial grain boundary dislocations at 8% shear strain. In previous work, we showed that the presence of vacancies and H impurities can make the nucleation process easier.

Defects in the boundary region can also be present due to deviations of the misorientation from that corresponding to the perfect CSL boundary. For the studies of glide velocities described in the next section, we first sheared the sample to the 8% shear that nucleated the dislocation pair. We then relaxed the applied stress and obtained a sample with the grain boundary dislocations in a stable configuration. Figure 3 shows the detail of the DSC lattice including one partial grain boundary dislocation in a stable configuration. The partial GB dislocation transforms the lowest energy structure into the secondary one. A second partial of opposite sign restores the lowest energy structure at the same original location. A second partial of the same sign restores the lowest energy structure at a plane below the original location.

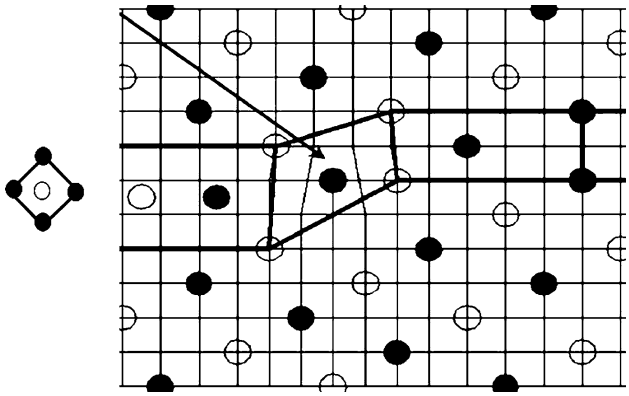

Fig. 3 The DSC lattice structure showing the partial GB dislocation that transforms the lowest energy structure into the secondary one. A second partial of opposite sign restores the lowest energy structure at the same original location. A second partial of the same sign restores the structure at a plane below the original location

Dislocation velocity

Starting from the sample containing the stable dislocation and no applied shear we increased the shear in small increments and measured the movement of the dislocation for various values of the applied shear. Dislocation positions as a function of time for the different values of applied shear are shown in Fig. 4. Figure 5 shows the dislocation velocities extracted from these simulations as a function of applied shear. It is seen that the Peierls barrier for these dislocations to glide corresponds to a shear strain between 1 and 1.5%. Using the bulk value of the shear modulus we obtain an estimate for the Peierls barrier of 0.0125 G or about 1 GPa. This is an upper bound to the actual Peierls barrier, since the effective shear modulus for the boundary region is lower than the bulk value [24].

The dynamic properties of dislocations are determined by the intrinsic properties of the dislocation in the crystal. At zero temperature, continuous glide motion of dislocations occurs only if the applied stress

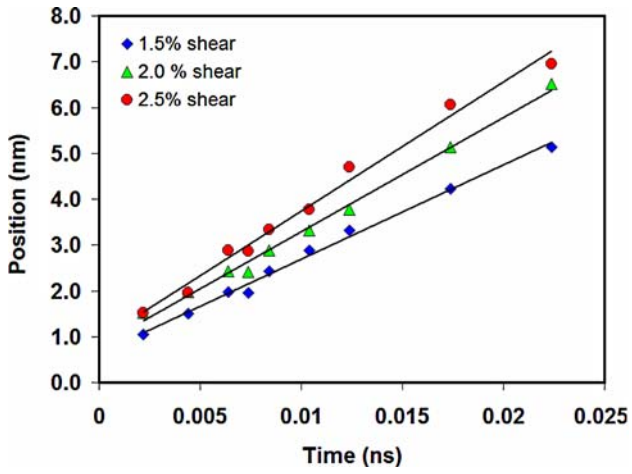

Fig. 4 Glide of a preexisting grain boundary dislocation for different levels of the applied shear strain

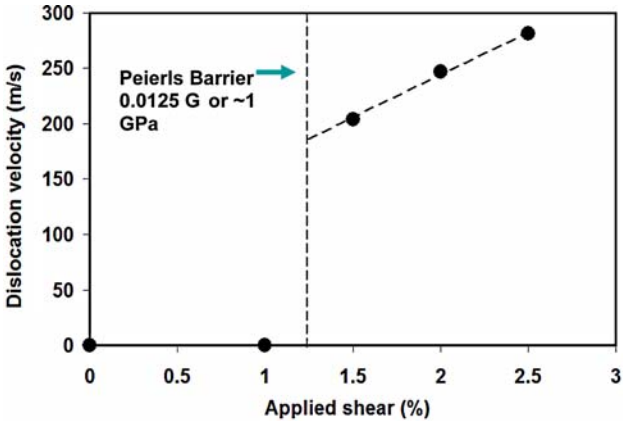

Fig. 5 Glide velocity of the grain boundary dislocation as a function of the applied shear strain

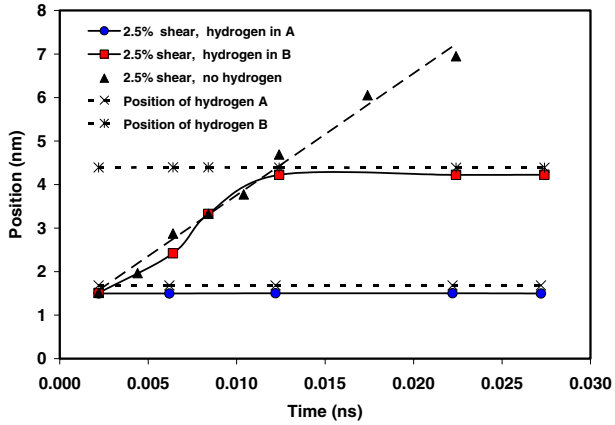

Fig. 6 Effect of a single hydrogen impurity atom on the glide of the grain boundary dislocation for an applied shear strain of 2.5%, showing that hydrogen stops dislocation glide

exceeds the Peierls barrier or maximum glide resistance. At finite temperatures however, macroscopic continuous glide of a dislocation can occur with the help of fluctuations at lower stresses.

In bcc metals, different regions for the dislocation velocity behavior have been postulated. In one region, the motion is controlled by the thermal fluctuations that release the dislocation from the equilibrium positions. This is the thermally activated region where the dislocation motion is jerky and depends on the applied stress in a highly non-linear manner. In a different regime, the drag resistance is predominant. The dependence of the velocity on stress is linear. The present results clearly fall in this latter regime. The results of Fig. 5 show that the dislocation velocity is linear with the applied shear. The magnitudes of the dislocation velocities obtained are similar to those found for lattice edge dislocations in bcc Mo by Chang, Bulatov and Yip [25, 26], that is on the order of 200–300 m/s for applied stresses of 1–2 GPa and a temperature of 77 K. The velocities obtained are lower than the velocity of sound in Fe, 4910 m/s at 300 K.

Effects of impurities and vacancies on dislocation glide

Figure 6 shows the dislocation response for an applied shear strain of 2.5% when a single H impurity is present. The figure shows the effects of the impurity present in two different locations, A and B. Position A is near the dislocation core and has the effect of impeding the start of the dislocation motion. Position B is along the slip plane but away from the initial position of the dislocation. The dislocation in this case starts moving and stops as it encounters the hydrogen impurity along its path. A similar effect was found when a carbon impurity was placed along the dislocation path. The dislocation stopped as it encountered the impurity, as shown in Fig. 7. A single vacancy was also placed in two different positions along the path of the gliding dislocation. The results are shown in Fig. 8, indicating that the vacancies do not have a significant effect on the motion of the dislocation.

Discussion and conclusions

The simulations presented here show that grain boundary dislocations can be the main mechanism by which grain boundary plasticity occurs. In analogy to lattice dislocations being the carriers of lattice plasticity, grain boundary dislocations can be the carriers of grain boundary plasticity. In addition, just as bulk plasticity may occur through partial lattice dislocations, grain boundary plasticity can occur through partial grain boundary dislocations. In the lattice, the area

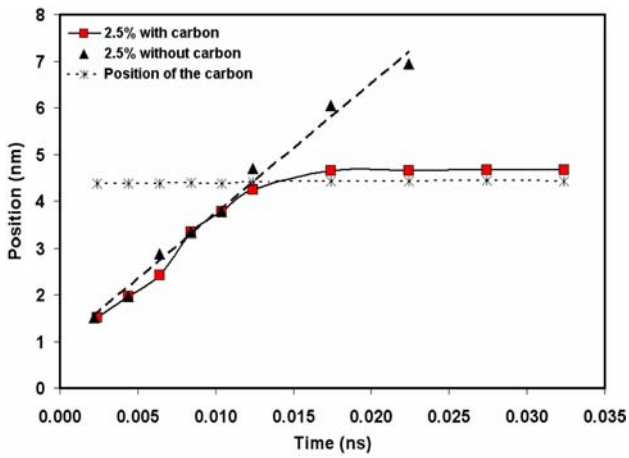

Fig. 7 Effect of a single carbon impurity atom on the glide of the grain boundary dislocation for an applied shear strain of 2.5%, showing that carbon stops dislocation glide

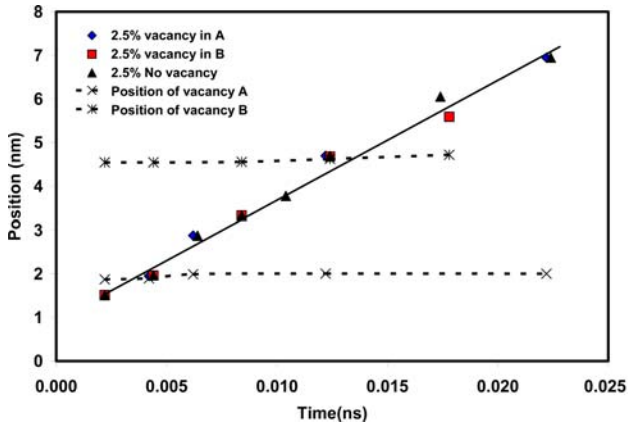

Fig. 8 Effect of a single vacancy on the glide of the grain boundary dislocation for an applied shear strain of 2.5%, showing that vacancies do not stops dislocation glide

between partial dislocations is an area characterized by a stacking fault, and in the case of partial grain boundary dislocations the area between them is an area where the grain boundary structure is an alternative grain boundary structure. In our results the difference in energy between the lowest energy structure and the alternative one is of the same order of magnitude as stacking faults in the lattice. Our simulations also show that these partial grain boundary dislocations can be nucleated in pairs, and can annihilate in a similar way as lattice dislocations. Partial grain boundary dislocations can glide in the grain boundary plane and this process results in migration of the boundary parallel to itself, intrinsically coupled to the sliding of the boundary.

The first simulation of this coupled motion was the pioneering work by Bishop et al., based on their molecular simulations using Lennard-Jones potential model. More recently, Cahn, Mishin and Suzuki [27] analyzed a series of boundaries, and have shown that this is a general phenomenon with the coupling coefficient being clearly linked to the crystallography of the grain boundary.

We have studied the dynamics of this process, which can be characterized simply as dislocation glide. The glide velocities that we have measured in our simulations are of the same order of magnitude expected for planar core edge dislocations in bcc metals. Although the nucleation of a pair of grain boundary dislocations requires a very high shear strain, we show that the glide of these grain boundary dislocations is characterized by a Peierls barrier, which corresponding to a shear strain between 1.25% and 1.5%.

The effect of impurities on the glide of the grain boundary dislocations, and therefore grain boundary sliding, is shown to be very significant. Two different interstitial impurities were studied, characterized by two different model potentials, mimicking the behavior of hydrogen and carbon. Both were shown to stop dislocation glide, indicating that impurities can decrease grain boundary sliding. This has very important implications for designing nanocrystalline materials with very high strengths. Vacancies that may be present on the grain boundary, on the contrary, did not have a significant effect on the movement of the dislocations. The effects of impurities and vacancies on the glide process are different from those found previously for the nucleation process [15]. For example, carbon impurities do not constitute a favored site for nucleation of the grain boundary dislocations but do play an important role in stopping glide once the dislocations are present.

Acknowledgements This work was supported by NSF, Materials Theory.

References

1. Van Swygenhoven H, Caro A Farkas D (2001) Scr Materialia 44(8–9):1513
2. Pond RC, Hirth JP (1994) Solid State Physics – Adv Res Appl 47:287
3. Van Swygenhoven H, Derlet PA (2001) Phys Rev B 64(22)
4. Hoagland RG, Kurtz R (2002) Philos Mag A – Phy Cond Matter Struct Defects Mech Prop 82(6):1073
5. Farkas D, Curtin WA (2005) MSE&A 412(1–2):316
6. Winning M (2004) Zeitschrift Fur Metallkunde 95(4):233
7. Kurtz RJ, Hoagland R, Hirth JP (1999) Philos Mag A – Phy Cond Matter Struct Defects Mech Prop 79(3):665
8. Sheikh Ali AD (1997) Acta Mater 45(8):3109
9. Sagalowic L, Clark WAT (1996) Interface Sci 4(1–2):29
10. Bollmann W (1981) Philos Mag A – Phy Cond Matter Struct Defects Mech Prop 43:201
11. Sansoz F, Molinari JF (2005) Acta Mater 53(7):1931
12. Dorfman S, Fuks D, Malbouisson LAC, et al (2003) Computational Mater Sci 27(1–2):199
13. Chandra N, Dang P (1999) J Mater Sci 34(4):655
14. Bishop GH Jr, Harrison R, Kwok T, Yip S (1982) J Appl Phys 53:5596
15. King TAH, Smith DA (1980) Acta Crystallogr A 36:335
16. Wang GJ, Sutton AP, Vitek V (1984) Acta Metallurgica 32(7):1093
17. Hyde B, Farkas D (2005) Philos Mag 85(32):3795
18. Geng WT, Freeman AJ, Wu R, Geller CB, Raynolds JE (1999) Phys Rev B 60:7149
19. Ballo P, Degmova J, Slugen V (2005) Phys Rev B 72(6)
20. Simonelli G, Pasianot R, Savino EJ (1993) Mater Res Soc 291:567
21. Ruda M, Farkas D, Abriata J (2002) Scr Materialia 46(5):349
22. Ruda M, Farkas D, Abriata J (1996) Phy Rev B 54(14):9765
23. Campbell GH, Kumar M, King WE, et al (2002) Philos Mag A – Phy Cond Matter Struct Defects Mech Prop 82(8):1573
24. Latapie A, Farkas D (2003) Scr Materialia 48(5):611
25. Chang JP, Bulatov VV, Yip S (1999) J Computer – Aided Mater Design 6(2–3):165
26. Chang JP, Bulatov VV, et al (2001) MSE&A 309:160
27. Cahn JW, Mishin Y, Suzuki A (2006) Philos Mag 86:3965